Inhibition of bacterial adhesion by epigallocatechin gallate attached polymeric membranes

Colloids and Surfaces B: Biointerfaces 221 (2023) 113024

Contents lists available at ScienceDirect

Colloids and Surfaces B: Biointerfaces

journal homepage: www.elsevier.com/locate/colsurfb

Inhibition of bacterial adhesion by epigallocatechin gallate attached polymeric membranes

Ömür Acet [a], Emrah Dikici [b], Burcu Önal Acet [b], Mehmet Odabaşı [b], Ivan Mijakovic [c,d], Santosh Pandit [c,*]

[a] Vocational School of Health Science, Pharmacy Services Program, Tarsus University, 33400 Tarsus, Mersin, Turkey
[b] Chemistry Department, Faculty of Arts and Science, Aksaray University, Aksaray, Turkey
[c] Department of Biology and Biological Engineering, Chalmers University of Technology, Kemivägen 10, 41296 Göteborg, Sweden
[d] Novo Nordisk Foundation Center for Biosustainability, Technical University of Denmark, Kongens Lyngby, Denmark

ARTICLE INFO

Keywords:
Staphylococcus aureus
Epigallocatechin gallate
Biofilms
Biomedical device

ABSTRACT

Microbial adhesion and formation of biofilms cause a serious problem in several areas including but not limited to food spoilage, industrial corrosion and nosocomial infections. These microbial biofilms pose a serious threat to human health since microbial communities in the biofilm matrix are protected with exopolymeric substances and difficult to eradicate with antibiotics. Hence, the prevention of microbial adhesion followed by biofilm formation is one of the promising strategies to prevent these consequences. The attachment of antimicrobial agents, coatings of nanomaterials and synthesis of hybrid materials are widely used approach to develop surfaces having potential to hinder bacterial adhesion and biofilm formation. In this study, epigallocatechin gallate (EGCG) is attached on p(HEMA-co-GMA) membranes to prevent the bacterial colonization. The attachment of EGCG to membranes was proved by Fourier-transform infrared spectroscopy (FT-IR). The synthesized membrane showed porous structure (SEM), and desirable swelling degree, which are ideal when it comes to the application in biotechnology and biomedicine. Furthermore, EGCG attached membrane showed significant potential to prevent the microbial colonization on the surface. The obtained results suggest that EGCG attached polymer could be used as an alternative approach to prevent the microbial colonization on the biomedical surfaces, food processing equipment as well as development of microbial resistant food packaging systems.

1. Introduction

The majority of healthcare associated infections are consequence of bacterial adhesion and biofilm formation especially on biomedical devices such as intravascular catheters, urinary catheters and orthopedic implants [1–3]. The formation of biofilms starts with adhesion of bacterial cell to surface and grow to build a community in a form of microcolonies, produce exopolymeric substances which not only act as structural backbone for biofilms but also protects the microbial communities from the antimicrobial agents as well as environmental assaults [4–6]. Hence, the strategies that can prevent the primary adhesion of bacterial cells to the surface of biomedical devices are attracting immense attention. Various chemical and physical strategies have been employed to prevent the microbial adhesion to biomedical devices. These strategies include surface modification, coatings of antibiotics or antimicrobial agents, incorporation of nanomaterials with strong antimicrobial behavior and antiadhesive coatings using passive polymers, hydrogel and zwitterionic polymers [7–14]. In addition to that covalent adhesion of quaternary ammonium cations, antimicrobial peptides, and molecules having strong potential of inhibiting bacterial quorum sensing are widely explored [15–19]. The physical strategies include the surface modification to achieve superhydrophobic characteristics which could prevent the bacterial colonization by superhydrophobic-hydrophobic interaction [20]. Most of these approaches except anti adhesive coatings are based on the bacteriostatic or bactericidal activity of coatings of antimicrobials or nanomaterials such as metallic nanoparticles. Although these coatings are efficient in terms of preventing biofilm formation, they potentially enhance the possibility of antimicrobial resistant development and undesired toxicity of host cells due to the release of metal ions from the metallic nanoparticles. Hence, search of novel antifouling strategy continues aiming for the development of surfaces which could repeal bacterial cells from

* Corresponding author.
E-mail address: pandit@chalmers.se (S. Pandit).

https://doi.org/10.1016/j.colsurfb.2022.113024

Available online 15 November 2022

surfaces, and efficiently prevent the bacterial colonization to biomedical devices while being harmless to human cells.

In this context, new high-performance polymeric materials have received much attention in the last few decades in biomedical applications such as wound healing and antibacterial studies, cancer diagnosis, synthetic organs, tissue engineering and drug carriers for controlled release etc [21–26]. The desired polymer selection depends on the type of membrane to be used, and the final application of the synthesized membrane [27]. Poly(hydroxyethyl methacrylate) (pHEMA)-based polymers, which are non-toxic and biocompatible ones with high water content and permeability, are extremely attractive polymeric networks [28]. They are among the major synthetic polymers and approved by FDA (Food and Drug Administration in the United States) for utilizing in biomedical, pharmaceutical, and industrial applications [29]. In the literature, there is a wide application area of pHEMA based materials in different forms. It has found wide usage area not only in the biomedical field, but also as a solid support material in different fields of both environment and biochemistry [30–34].

The modification of the membrane surface lets its properties to be improved while retaining the intrinsic bulk features, and imparting the valuable properties of material at the nanoscale to the membrane construction [35]. It is well known that pure polymeric materials usually cannot be utilized in all areas for high performance applications without being modified [36]. The real significance of a modification is that it provides a technique to improve surface properties while maintaining the original matrix efficiency. Surface modification techniques of polymeric materials can be divided into physical and chemical methods. Chemical methods may be preferred to physical ones because covalent bonding provides long-term chemical stability [37].

The epigallocatechin gallate (EGCG) is a constituent of polyphenols abundantly present in tea extract and shown to have broad range of antimicrobial behavior while being harmless to human cells [38,39]. The potential of EGCG to prevent the biofilm formation has been demonstrated by previous studies [38–40]. The inhibitory effect of EGCG to disrupt the quorum sensing of bacterial cells has been suggested as a key mechanism to prevent the bacterial colonization to surfaces followed by the biofilm formation [40]. To utilize the excellent anti-biofilm efficiency of EGCG, the molecules was attached to p (HEMA-co-GMA) membranes as functional active molecules to prevent the microbial adhesion. Synthesized membranes were characterized by FTIR, SEM and surface contact angle devices to get some important information about functional groups, surface morphology and surface hydrophilicity of the membrane. The potential of membranes to prevent microbial adhesion were tested against *S. aureus*. The obtained results in this study demonstrate the antiadhesion potential of EGCG attached polymeric membranes which can be potentially utilized in the biomedical devices or food packaging systems to prevent the microbial attachment.

2. Materials and methods

2.1. Materials

2-Hydroxyethyl methacrylate (HEMA) and *N,N,N´N´*-tetramethylethylene diamine (TEMED) were obtained from Fluka A.G (Buchs, Switzerland). Glycidyl methacrylate, *N,N´*-methylene-bis-acrylamide (MBAm), ammonium persulfate (APS), and other chemicals having reagent grade were purchased from Sigma (St. Louis, MO, USA). Used water during experiments was purified with a Barnstead ROpure LP® reverse osmosis unit (Dubuque, IA, USA). The (-)-epigallocatechin gallate (EGCG) was purchased from sigma Aldrich (Sweden).

2.2. Synthesis of p(HEMA-co-GMA) membranes

HEMA and GMA monomers (each as 850 μL) were taken into the falcon tube. Next, 0.5 mL of MBAAm solution (20 mg/mL in ethanol) was added to the monomer solution as a crosslinker. In addition, 0.5 mL of ethanol was added to the monomer mixture to create a porous structure in the membrane. After adding 0.5 mL APS (0.1 g/mL in dH_2O) and 50 μL TEMED solutions as initiator and as catalyst, respectively into the monomer mixture. The acquired mixture was vortexed for 1 min to obtain a homogenous media. This prepared mixture was poured into a glass petri dish with a diameter of 2.5 cm. After the lid was closed, it left at room conditions for 1 day to complete polymerization. In order to remove non-polymerized residues from the synthesized membrane, it was washed several times with EtOH-dH_2O (50:50), and dH_2O. It was checked whether the washing process was completed with a UV spectrophotometer.

2.3. Attachment of epigallocatechin gallate to p(HEMA-co-GMA) membranes

For this, epigallocatechin gallate (EGCG) solutions were prepared at concentrations of 100, 200, 400, 600, 1000 μg/mL with 0.05 M carbonate buffer at pH 11. Then, the synthesized membranes were wetted in 0.05 M carbonate buffer of pH 11 for equilibration for 2 h. And finally, certain amounts of equilibrated membranes were treated with different concentrations of EGCG solutions of 20 mL for 2 h for attaching EGCG molecules. In order to remove non-reacted residues from the membranes, they were washed several times with dH_2O. A spectrophotometric method was used to determine the amount of EGCG bound to the membrane surface [41,42]. According to this method, the pre- and post-reaction concentrations of EGCG solutions were determined spectrophotometrically at 275 nm.

In order to calculate the amount of EGCG bound to the surface of the membranes, the difference between the concentration of the initial and post-reaction (including washing solutions) solutions of EGCG was computed by using Eq. 1.

$$q = \frac{(C_i - C_f) \times V}{m} \quad (1)$$

Here, q presents the amount of bound EGCG per gram (μg/g). C_i and C_f represent the EGCG concentrations (μg/mL) for initial and final solutions, respectively. V is the solution volume (mL), and m is the weight of the membrane used (g).

Methods such as elemental analysis and FTIR are also used to determine the amount of active molecule bound to a polymeric surface. However, certain conditions must be provided for the implementation of these methods to calculate the concentration of active molecules on the membrane. For example, in order to establish a stoichiometric equation in the use of elemental analysis, different atoms must be present in the polymeric structures and the bonded molecules. In this study, elemental analysis method could not be used because the atoms in the polymeric membrane and EGCG structures are similar. In the case of non-homogeneous distribution of the active molecules attached to the surface, the use of FTIR method for quantitative analysis may not give accurate results. Against such analysis risks, it should be emphasized that active substance determination in initial and final solution for the quantification of attached molecule on the membrane used in this study is more reliable.

A putative representation of EGCG attachment on p(HEMA-co-GMA) membrane is shown in Fig. 1.

2.4. Characterization of p(HEMA-co-GMA) membranes

Synthesized p(HEMA-co-GMA) based membranes were characterized to investigate their functional groups and surface morphology by using fourier transform infrared (FTIR) instrument (Perkin Elmer, Spectrum 100, USA), multipoint Brunauer–Emmett–Teller (BET) method (Quantachrome, Nova 2200E, USA), and scanning electron microscopy (SEM, EVO LS 10 ZEISS 5600 SEM, Tokyo, Japan) devices respectively.

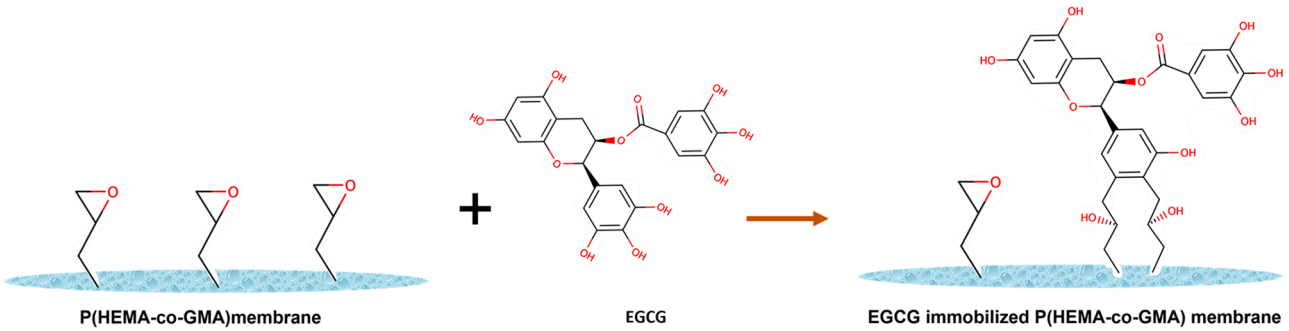

Fig. 1. Attachment reaction of epigallocatechin gallate on p(HEMA-co-GMA) membrane.

In addition, the synthesized p(HEMA-co-GMA) based membranes were also tested for free and bound water content to calculate their porosity. For this aim first, the water-saturated membranes were placed in a known volume of deionized water in a graduated vessel, and the volume change obtained before (V_b) and after (V_a) addition of the membranes was calculated (i.e., $V_o = V_a - V_b$). The water-saturated membranes (m_w) were subjected to two types of tests. In the first test, the water in the swollen membranes was squeezed between two fingers and the weights (m_s) of the compressed membranes were recorded, and the free water content (*FWC*) (porosity) of the membranes was calculated from Eq. 2. Here, ρ is the density of water.

$$FWC = \frac{m_w - m_s}{\rho_w V_o} x100 \quad (2)$$

For calculation of total water content of the membrane, the following Eq. 3 is used. Here m_d is weight of membranes dried in an oven at 60 °C.

$$TWC = \frac{m_w - m_d}{\rho_w V_o} x100 \quad (3)$$

Water content bound inner and outer surface of the membrane was computed from difference of two equations.

Contact angle measurement studies of plane and 100 μg/mL EGCG attached p(HEMA-co-GMA) membranes were tested using the Krüss DSA100 (Hamburg, Germany) device. For this aim, 1 drop of dH_2O was added on the synthesized p(HEMA-co-GMA) membrane surface, and contact angles were taken with the sessile drop method. At least 10 different photographs were recorded from different parts of the membrane surface, and an average value was computed.

2.5. Biofilm formation assay

Control and EGCG attached membranes were cut to achieve a piece of 0.7 × 0.7 cm. The antibiofilm potential of EGCG attached membranes was evaluated against *S. aureus* CCUG 10778. The overnight grown *S. aureus* culture was diluted to fresh tryptic soy broth to obtain a final inoculum of 2–5 × 10^6 CFU/mL. To grow biofilm, pieces of control and EGCG attached membranes were placed in 24 well plate containing 1 mL of inoculum, and incubated for 4 h and 24 h at 37 °C. After respective time of bacterial growth, surfaces were dip-rinsed with sterile water and collected in 0.89% of NaCl to evaluate the number of adhered bacterial cells. The colonized bacterial cells in membranes were removed and homogenized by sonication (15 s; 10% of amplitude). The homogenized solution was serially diluted and plated in agar plates to count the colony forming unites (CFUs). The bacterial adhesion to membranes were further examined by scanning electron microscope as described previously [43]. Briefly, after 4 h and 24 h of bacterial growth, adhered bacterial cells on membranes were fixed using 3% of glutaraldehyde for 2 h. The fixed samples were dehydrated using graded series of ethanol (40, 50, 60, 70, 80, and 90 v/v%) each for 10 min and with 100 v/v% for 15 min. The dehydrated samples were dried at room temperature for overnight and sputter coated with gold (5 nm). The SEM images were acquired using JEOL JSM 6301 F (Carl Zeiss AG, Jena, Germany). Furthermore, the density of live and dead bacterial cells on membrane surfaces was examined by using fluorescence microscopy as described previously [44]. Briefly, the bacterial cells adhered on the surfaces (after 4 h of growth) were stained with the mixture of 6.0 μM SYTO 9 and 30 μM potassium iodide from Live/Dead BacLight Viability kit L13152 (Invitrogen, Molecular Probes, Inc. Eugene, OR, USA). Fluorescence microscopic images of the stained biofilms were acquired by using a Zeiss fluorescence microscope (Axio Imager.Z2m Carl Zeiss, Jena, Germany). The acquired images were further analyzed for the quantification of different color intensities using ImageJ (National Institute of Health).

2.6. Statistical analysis

All data are presented as the mean ± standard deviation from at least three different biological replicates. Intergroup differences were estimated by one-way analysis of variance (ANOVA), followed by a post hoc multiple comparison (Tukey) test to compare the multiple means. Differences between values were considered statistically significant when the *P*-value was < 0.05.

3Results and discussions

3.1. Characterization of p(HEMA-co-GMA) membranes

FT-IR spectra studied for both characteristic functional groups of p (HEMA-co-GMA) membranes, and EGCG attached ones are given in Fig. 2. The FT-IR spectra of plain membrane, the membranes treated with the lowest and highest concentration of EGCG are shown in Fig. 2A and B, C, respectively. Here, some useful characteristic infrared bands for aromatic compounds were observed. The C–H stretching bands of aromatic EGCG appear around 3000 cm^{-1}. Aromatic C═C stretching bands in skeletal vibrations are seen around 1450 cm^{-1}. Bands around 920 cm^{-1} were attributed to C-O groups in epoxy molecules in plain membranes. And, as the amount of EGCG attaching onto membrane increased, the amount of epoxy groups decreased. Bands between 1700 and 1730 cm^{-1} are due to stretching of C═O groups of the both plain membrane and EGCG. O-H groups produce their characteristic bands around 3500–3600 cm^{-1}. All obtained data approved that EGCG molecules were attached to p(HEMA-co-GMA) membranes successfully.

p(HEMA-co-GMA) membranes were also characterized by using SEM to get some important knowledge about surface morphology and membrane structures. The represented SEM images are shown in Fig. 3 with different levels of magnification.

As seen from the surface (Fig. 3A-F), synthesized membranes have a porous structure, which is a desirable feature for membranes, especially

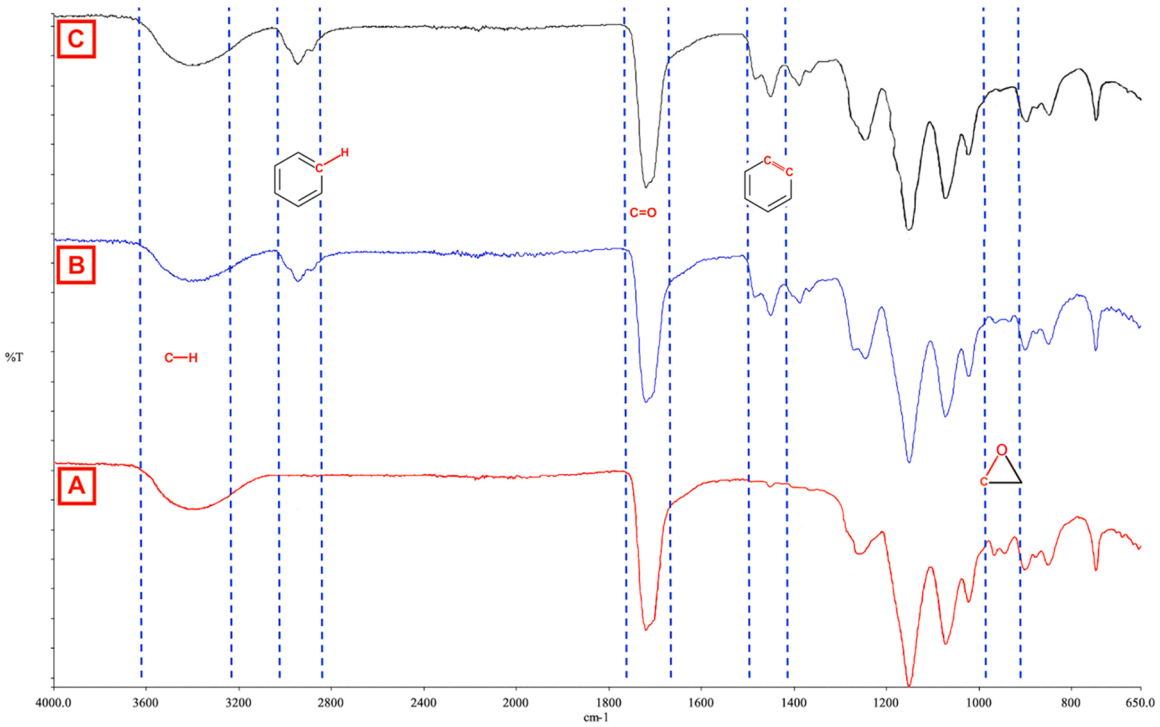

Fig. 2. The FTIR spectra of p(HEMA-co-GMA) (A), and p(HEMA-co-GMA) membranes treated with EGCG at a concentration of 100 (B) and 1000 (C) μg/mL, respectively.

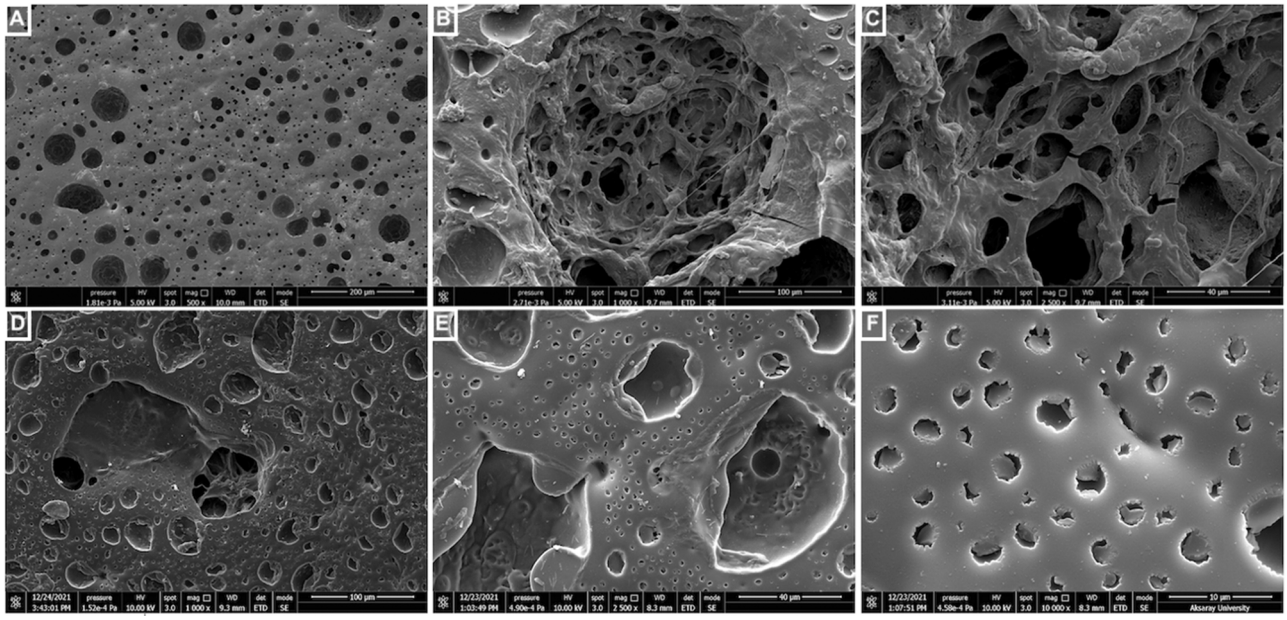

Fig. 3. SEM micrographs of p(HEMA-co-GMA) membranes with different magnifications.

when they are used for therapeutic purposes [23]. In addition, p(HEMA-co-GMA) membranes synthesized in this study have small pores mostly in the range of 3–10 μm (Fig. 3F), and this feature gives the membranes a large surface area for active substance binding, high water retention and mechanical strength [45,46]. The internal pore structure of the synthesized membranes is also given in Fig. 3B and C. As can be seen from these microphotographs, the internal structures of the membranes also have super-porous structures which increase the usable area of the polymer [47]. For porosity investigation, free water content (porosity) and the total water content of the synthesized p(HEMA-co-GMA) membranes were evaluated using deionized water and found as 71% and 81%, respectively. These results suggest that 71% of the total volume of the synthesized membranes consists of macropores and 10% of the volume is micropores [48]. According to BET analysis, the specific surface area of the p(HEMA-co-GMA) membranes was determined as 47 m^2/g. The contact angle value gives information about the hydrophilicity of the surface. Contact angle measurements of plane and EGCG (100 μg/mL) attached p(HEMA-co-GMA) membranes are given in Fig. 4.

Surfaces with contact angle degree between 0 and 90° show

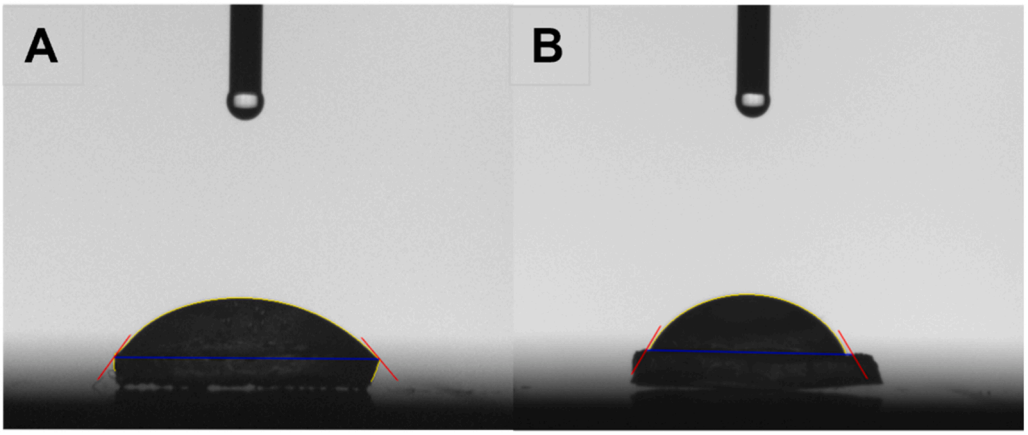

Fig. 4. Contact angle measurements of plane p(HEMA-co-GMA) (A) and EGCG attached p(HEMA-co-GMA) (B) membranes. Data is the average of 3 measurements.

hydrophilic character. Surface hydrophilicity decreases as the contact angle approaches 90º. And surface shows hydrophobic character over 90º. As seen from Fig. 4, contact angle values for plane and EGCG (100 μg/mL) attached p(HEMA-co-GMA) membranes were obtained to be 52.3º ± 0.5 and 59.1º ± 0.7, respectively. There was a 13% increase in the surface contact angle of the membrane interacting with EGCG at a concentration of 100 μg/mL. This enhancement in hydrophobicity may be due to the presence of aromatic groups on EGCG molecules which are attached to membrane surface.

3.2. Studies to prevent bacterial colonization of EGCG attached p(HEMA-co-GMA) membranes

The antibacterial efficiency of EGCG attached membranes was examined by evaluating the numbers of colonized bacterial cells in terms of CFUs, scanning electron microscopy and fluorescence microscopy analysis. Since the potential of EGCG for biofilm formation is widely accepted, EGCG was attached on p(HEMA-co-GMA) membrane to develop antifouling surfaces. The antiadhesion potential of membranes with different concentrations of EGCG were tested against a Gram-positive bacterium *S. aureus*. *S. aureus* was chosen in this study since it is the most common opportunistic pathogen to cause nosocomial infections, and widely used as a model Gram positive bacterium for biofilm studies. The concentration of free EGCG > 50 μg/mL in solution was demonstrated previously to efficiently inhibit the biofilm formation by *S. aureus* [49]. Hence ≥ 100 μg/mL of EGCG was attached on p(HEMA-co-GMA) membranes in order to achieve higher efficiency to prevent the bacterial colonization.

As shown in Fig. 5, the extent of *S. aureus* colonization was found to be significantly reduced on EGCG attached p(HEMA-co-GMA) membrane, compared to bare p(HEMA-co-GMA) membrane. The percentage of *S. aureus* adhesion was observed to be correlated with the concentration of attached EGCG. Specifically, the colonization of *S. aureus* was inhibited in a fraction of 25.9 ± 17.2%, 35.4 ± 12.3%, 47.1 ± 5.2%, 58.6 ± 4.8% and 71.0 ± 4.5% on surfaces of 100 μg/mL, 200 μg/mL, 400 μg/mL, 600 μg/mL and 1000 μg/mL of EGCG attached p(HEMA-co-GMA) membrane in compared to control samples after 4 h of bacterial growth (Fig. 5A). Whereas 11.6 ± 7.6%, 24.1 ± 3.1%, 38.1 ± 5.9%, 51.2 ± 5.8% and 62.5 ± 4.0% of inhibition in *S. aureus* colonization was observed respectively on surfaces of 100 μg/mL, 200 μg/mL, 400 μg/mL, 600 μg/mL and 1000 μg/mL of EGCG attached p(HEMA-co-GMA) membrane in compared to control samples after 24 h of bacterial growth (Fig. 5B). Considering the specific surface areas of the membranes, and the different EGCG concentrations in the reaction medium, the amounts of EGCG attached to the membranes were found to be 3.65 mg/g, 8.72 mg/g, 19.30 mg/g, 31.82 mg/g and 35.62 mg/g, respectively. As seen here, amount of EGCG attached to membrane was increased as the parallel to concentration of EGCG in the media. In order to confirm the results obtained from CFUs counting, the membranes were examined under SEM after 4 h and 24 h of bacterial growth. The representative SEM images clearly demonstrate the significantly reduced density of *S. aureus* colonization on the EGCG attached polymer surfaces after both 4 h and 24 h of bacterial growth in compared respective control (Fig. 6A & 6B). The surface of p(HEMA-co-GMA) membrane without EGCG is mostly covered with adhered bacterial cell in the form of microcolonies even with the 4 h of bacterial growth

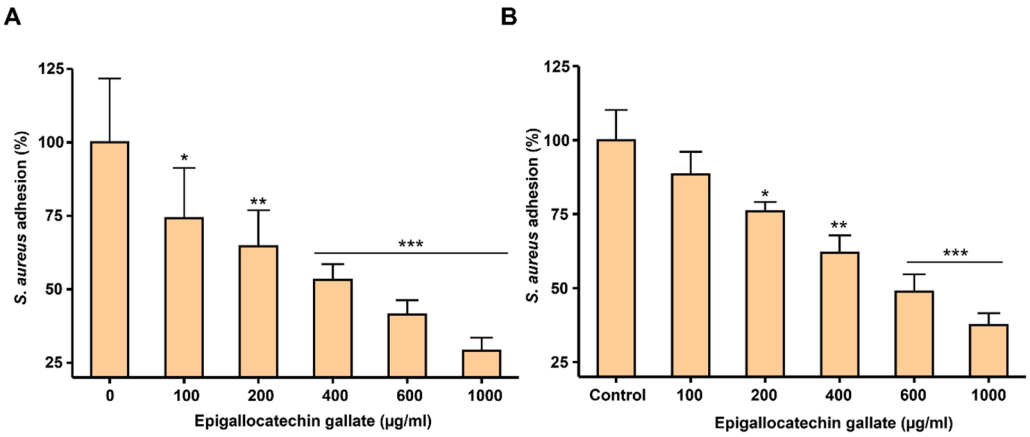

Fig. 5. Efficiency of EGCG attached p(HEMA-co-GMA) membrane against *S. aureus* adhesion after 4 h (A) and 24 h (B) of growth. Data represents mean ± standard deviation of three independent biological replicates. * $P < 0.05$, ** $P < 0.001$, *** $P < 0.0001$.

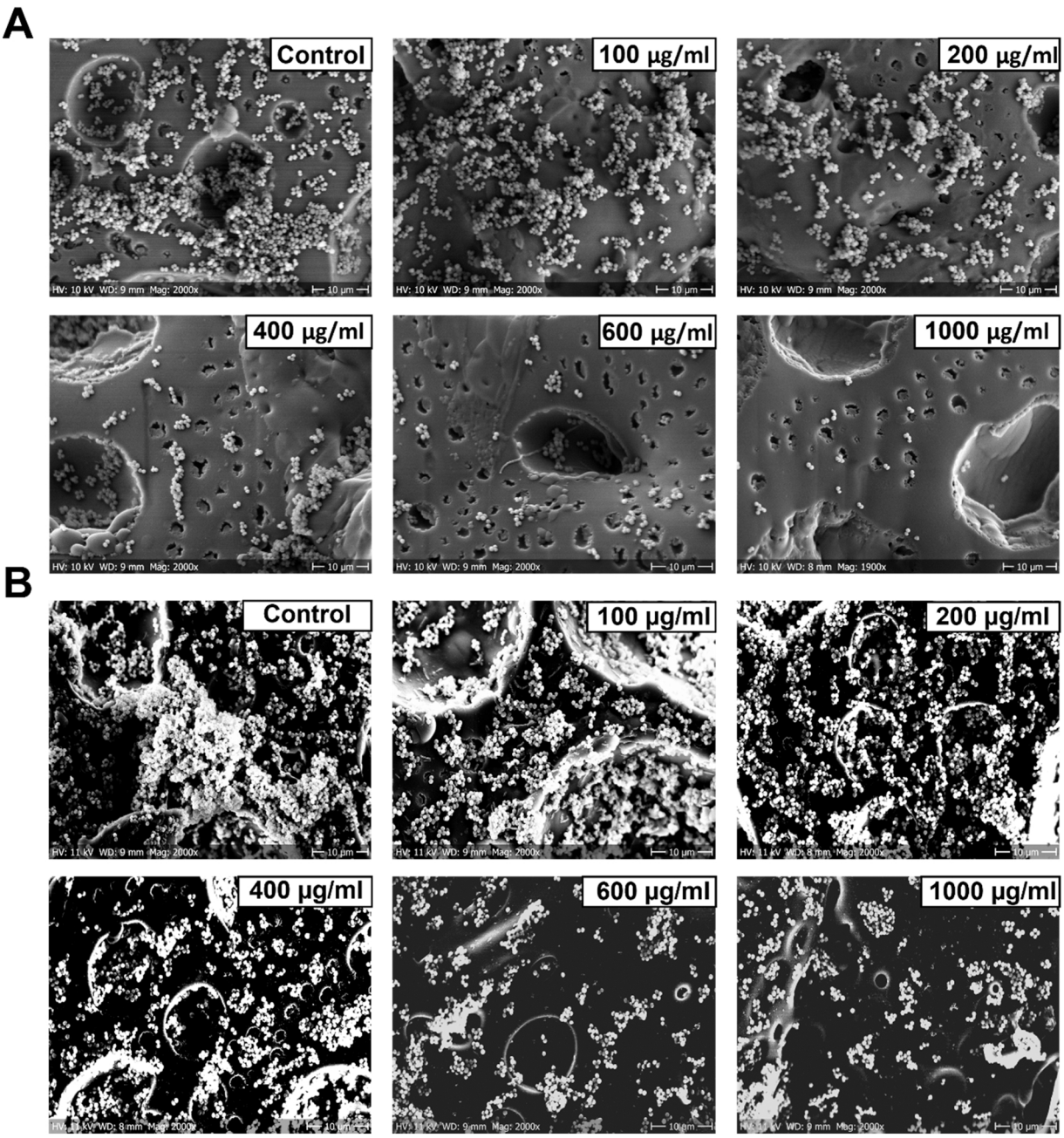

Fig. 6. Representative SEM images depicting bacterial colonization on the surface of control and different concentrations of EGCG attached p(HEMA-co-GMA) membrane after 4 h (A) and 24 h (B) of bacterial culture.

(Fig. 6A). The reduced numbers of bacterial cells, and lesser extent of microcolonies can be seen in 100 µg/mL, 200 µg/mL of EGCG attached polymer surface in compared to control. Whereas a dramatic decrease in adhered bacteria and very few microcolonies are observed at 400 µg/mL and 600 µg/mL of EGCG attached polymer surface. As expected, very few bacterial adhesions were observed on the surface of 1000 µg/mL of EGCG attached polymer surface. Interestingly, on the 1000 µg/mL of EGCG attached surface, the adhered cells are found independent instead of aggregated cells or formation of microcolonies, suggesting the strong antiadhesion efficiency. The significant reduction in bacterial attachment was observed at the $\geq$ 200 µg/mL of EGCG attached polymer surfaces after 24 h of bacterial growth (Fig. 6B). After 24 h of bacterial growth, the polymer surface without EGCG (control) was mostly filled with densely packed microcolonies. Whereas decrease in density of bacterial cells and microcolonies was detected with the increasing concentration of EGCG on the polymer surface (Fig. 6B). Simply put, the results from SEM analysis are consistent with the result obtained from CFUs counting.

Although in general EGCG has been shown to be bacteriostatic and efficient in preventing the biofilm formation by inhibiting the quorum sensing regulator at lower concentrations, higher concentrations have been suggested to be bactericidal [38,40,50]. Hence, to elucidate how EGCG attached p(HEMA-co-GMA) membrane is preventing the microbial colonization, the colonized cells were stained with live/dead viability stain and examined under fluorescence microscope. Fig. 7A shows the representative fluorescence microscopic images depicting the strong inhibitory efficiency of EGCG attached membrane on the bacterial colonization after 4 h of bacterial culture. The acquired fluorescence images were quantified and presented in Fig. 7B. Like SEM results, decreasing density of bacterial cells was observed on the membrane

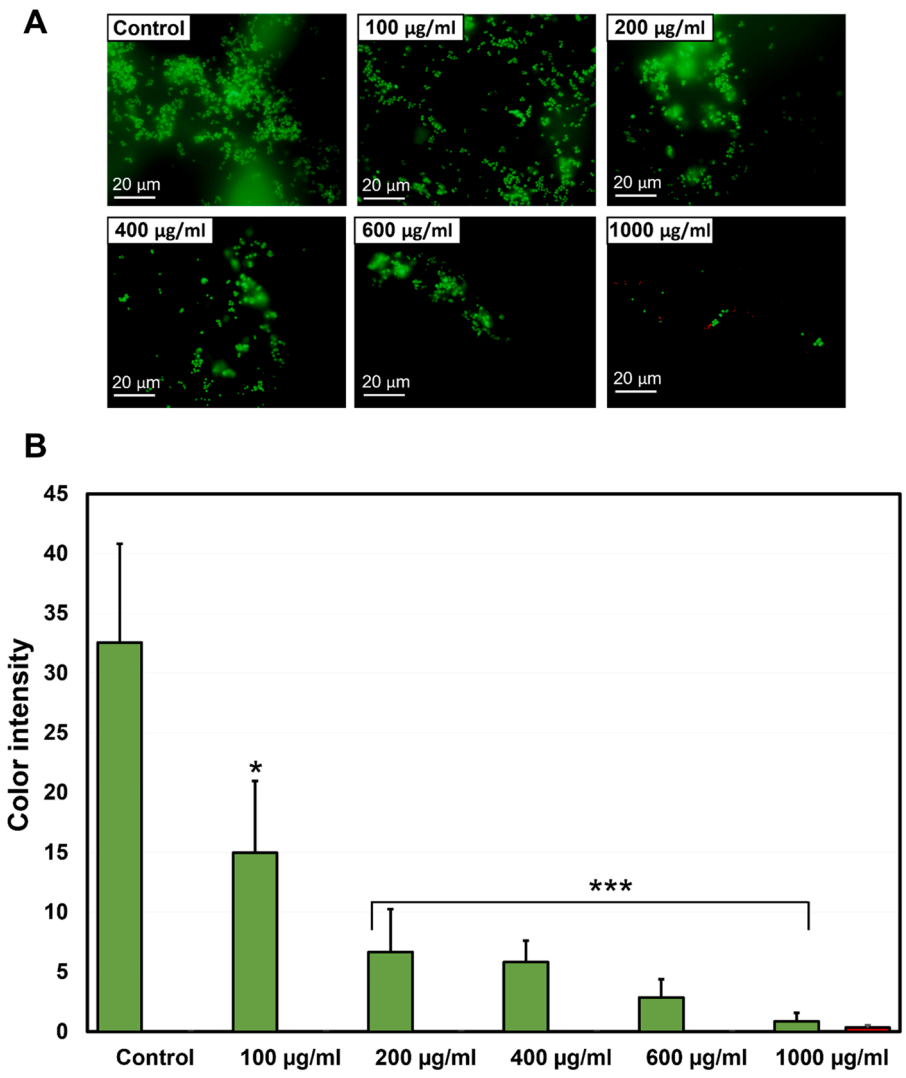

Fig. 7. Representative fluorescence microscopic images depicting the bacterial colonization and live-dead bacteria on control and different concentrations of EGCG attached p(HEMA-co-GMA) membrane (A). Green color denotes live bacteria and red color denotes dead bacterial cells. (B) Quantification of fluorescence color intensity of images acquired from live/dead viability staining.

surface having higher concentrations of EGCG. The lesser extent of bacterial aggregation and fewer microcolonies were found on the surface of higher concentrations of EGCG attached membranes in compared to control membranes. Interestingly, no dead bacterial cells were found on the membrane surfaces with EGCG at concentrations of 600 µg/mL or less, suggesting that observed inhibition in microbial colonization is not associated to bactericidal activity. However, a few dead cells were observed at 1000 µg/mL of EGCG attached surfaces (Fig. 7A & 7B). This observation suggests that polymer surface having higher concentration of attached EGCG not only prevents the microbial colonization but also could deactivate the attached bacterial cells.

4. Conclusion

In summary, various concentrations of EGCG were successfully attached on p(HEMA-co-GMA) membrane. The obtained result in this study suggests that the right concentration of EGCG attached to polymer surfaces can strongly enhance the antiadhesion properties of the surface and prevent bacterial colonization. To the best of our knowledge, this is the first demonstration on the possibility of EGCG attachment on p (HEMA-co-GMA) membrane surface to prevent the adhesion of bacterial cells. This observation could be useful to design new polymer based biomedical devices with the ability to prevent the bacterial colonization. In addition to that it could also provide a new insight on the development of microbial resistant polymer surfaces.

CRediT authorship contribution statement

Ömür Acet: Conceptualization, Methodology, Formal analysis, Investigation, Writing – original draft. **Emrah Dikici**: Formal analysis, Investigation. **Burcu Önal Acet**: Formal analysis, Investigation. **Mehmet Odabaşi**: Formal analysis, Review and editing. **Ivan Mijakovic**: Formal analysis, Review and editing. **Santosh Pandit**: Conceptualization, Methodology, Formal analysis, Investigation, Writing – original draft, Review and editing.

Declaration of Competing Interest

The authors declare that they have no known competing financial interests or personal relationships that could have appeared to influence the work reported in this paper.

Data availability

Data will be made available on request.

Acknowledgment

This work was performed in part at Myfab Chalmers.

Funding

This work was supported by Vetenskapsrådet to SP, NordForsk, the Independent Research Fund Denmark - FNU and NNF20CC0035580 to IM.

References

[1] K.G. Neoh, M. Li, E.T. Kang, E. Chiong, P.A. Tambyah, Surface modification strategies for combating catheter-related complications: recent advances and challenges, J. Mater. Chem. B 5 (2017) 2045–2067.
[2] Z. Khatoon, C.D. McTiernan, E.J. Suuronen, T.F. Mah, E.I. Alarcon, Bacterial biofilm formation on implantable devices and approaches to its treatment and prevention, Heliyon 4 (2018), e01067.
[3] N.C. Dadi, B. Radochová, J. Vargová, H. Bujdáková, Impact of healthcare-associated infections connected to medical devices—an update, Microorganisms 9 (2021) 2332.
[4] H.C. Flemming, J. Wingender, U. Szewzyk, P. Steinberg, S.A. Rice, S. Kjelleberg, Biofilms: an emergent form of bacterial life, Nat. Rev. Microbiol. 14 (2016) 563–575.
[5] W. Yin, Y. Wang, L. Liu, J. He, Biofilms: the microbial “protective clothing” in extreme environments, Int. J. Mol. Sci. 20 (2019) 3423.
[6] A.J. Paula, G. Hwang, H. Koo, Dynamics of bacterial population growth in biofilms resemble spatial and structural aspects of urbanization, Nat. Commun. 11 (2020) 1–4.
[7] C.J. Huang, L.C. Wang, C.Y. Liu, A.S. Chiang, Y.C. Chang, Natural zwitterionic organosulfurs as surface ligands for antifouling and responsive properties, Biointerphases 9 (2014), 029010.
[8] D. Li, P. Lv, L. Fan, Y. Huang, F. Yang, X. Mei, D. Wu, The immobilization of antibiotic-loaded polymeric coatings on osteoarticular Ti implants for the prevention of bone infections, Biomater. Sci. 5 (2017) 2337–2346.
[9] P. Singh, S. Pandit, J. Garnæs, S. Tunjic, V.R. Mokkapati, A. Sultan, A. Thygesen, A. Mackevica, R.V. Mateiu, A.E. Daugaard, A. Baun, I. Mijakovic, Green synthesis of gold and silver nanoparticles from *Cannabis sativa* (industrial hemp) and their capacity for biofilm inhibition, Int. J. Nanomed. 13 (2018) 3571–3591.
[10] S. Pandit, K. Gaska, V.R.S.S. Mokkapati, S. Forsberg, M. Svensson, R. Kadar, I. Mijakovic, Antibacterial effect of boron nitride flakes with controlled orientation in polymer composites, RSC Adv. 9 (2019) 33454–33459.
[11] S. Pandit, K. Gaska, V.R.S.S. Mokkapati, E. Celauro, A. Derouiche, S. Forsberg, M. Svensson, R. Kadar, I. Mijakovic, Precontrolled alignment of graphite nanoplatelets in polymeric composites prevents bacterial attachment, Small 16 (2020) 1904756.
[12] P. Sautrot-Ba, N. Razza, L. Breloy, S.A. Andaloussi, A. Chiappone, M. Sangermano, C. Hélary, S. Belbekhouche, T. Coradin, D.L. Versace, Photoinduced chitosan–PEG hydrogels with long-term antibacterial properties, J. Mater. Chem. B 7 (2019) 6526–6538.
[13] S.A. Jalil, M. Akram, J.A. Bhat, J.J. Hayes, S.C. Singh, M. ElKabbash, C. Guo, Creating superhydrophobic and antibacterial surfaces on gold by femtosecond laser pulses, Appl. Surf. Sci. 506 (2020), 144952.
[14] A. Uneputty, A. Dávila-Lezama, D. Garibo, A. Oknianska, N. Bogdanchikova, J. F. Hernández-Sánchez, A. Susarrey-Arce, Strategies applied to modify structured and smooth surfaces: a step closer to reduce bacterial adhesion and biofilm formation, Colloid Interface Sci. Commun. 46 (2022), 100560.
[15] K.K. Ho, R. Chen, M.D. Willcox, S.A. Rice, N. Cole, G. Iskander, N. Kumar, Quorum sensing inhibitory activities of surface immobilized antibacterial dihydropyrrolones via click chemistry, Biomaterials 35 (2014) 2336–2345.
[16] D. Druvari, N.D. Koromilas, G.C. Lainioti, G. Bokias, G. Vasilopoulos, A. Vantarakis, I. Baras, N. Dourala, J.K. Kallitsis, Polymeric quaternary ammonium-containing coatings with potential dual contact-based and release-based antimicrobial activity, ACS Appl. Mater. Interfaces 8 (2016) 35593–35605.
[17] A. Andrea, N. Molchanova, H. Jenssen, Antibiofilm peptides and peptidomimetics with focus on surface immobilization, Biomolecules 8 (2018) 27.
[18] P. Prateeksha, R. Bajpai, C.V. Rao, D.K. Upreti, S.K. Barik, B.N. Singh, Chrysophanol-functionalized silver nanoparticles for anti-adhesive and anti-biofouling coatings to prevent urinary catheter-associated infections, ACS Appl. Nano Mater. 4 (2021) 1512–1528.
[19] L. Stillger, D. Müller, Peptide-coating combating antimicrobial contaminations: a review of covalent immobilization strategies for industrial applications, J. Mater. Sci. 57 (2022) 10863–10885.
[20] Y. Yuan, M.P. Hays, P.R. Hardwidge, J. Kim, Surface characteristics influencing bacterial adhesion to polymeric substrates, RSC Adv. 7 (2017) 14254–14261.
[21] X. Liu, T. Lin, J. Fang, G. Yao, H. Zhao, M. Dodson, X. Wang, In vivo wound healing and antibacterial performances of electrospun nanofibre membranes, J. Biomed. Mater. Res. A 94 (2010) 499–508.
[22] N. Geisel, J. Clasohm, X. Shi, L. Lamboni, J. Yang, K. Mattern, G. Yang, K. H. Schäfer, M. Saumer, Microstructured multilevel bacterial cellulose allows the guided growth of neural stem cells, Small 12 (2016) 5407–5413.
[23] A.T. Iacob, M. Drăgan, N. Gheţu, D. Pieptu, C. Vasile, F. Buron, S. Routier, S. E. Giusca, I.D. Caruntu, L. Profire, Preparation, characterization and wound healing effects of new membranes based on chitosan, hyaluronic acid and arginine derivatives, Polymers 10 (2018) 607.
[24] S. Li, A. Jasim, W. Zhao, L. Fu, M.W. Ullah, Z. Shi, G. Yang, Fabrication of pH-electroactive bacterial cellulose/polyaniline hydrogel for the development of a controlled drug release system, ES Mater. Manuf. 1 (2018) 41–49.
[25] M. Ul-Islam, F. Subhan, S.U. Islam, S. Khan, N. Shah, S. Manan, M.W. Ullah, G. Yang, Development of three-dimensional bacterial cellulose/chitosan scaffolds: analysis of cell-scaffold interaction for potential application in the diagnosis of ovarian cancer, Int. J. Biol. Macromol. 137 (2019) 1050–1059.
[26] L. Wang, S. Hu, M.W. Ullah, X. Li, Z. Shi, G. Yang, Enhanced cell proliferation by electrical stimulation based on electroactive regenerated bacterial cellulose hydrogels, Carbohydr. Polym. 249 (2020), 116829.
[27] G.M. Geise, H.S. Lee, D.J. Miller, B.D. Freeman, J.E. McGrath, D.R. Paul, Water purification by membranes: the role of polymer science, J. Polym. Sci. B Polym. Phys. 48 (2010) 1685–1718.
[28] M. Zare, A. Bigham, M. Zare, H. Luo, E. Rezvani Ghomi, S. Ramakrishna, pHEMA: an overview for biomedical applications, Int. J. Mol. Sci. 22 (2021) 6376.
[29] S. Atzet, S. Curtin, P. Trinh, S. Bryant, B. Ratner, Degradable poly (2-hydroxyethyl methacrylate)-co-polycaprolactone hydrogels for tissue engineering scaffolds, Biomacromolecules 9 (2008) 3370–3377.
[30] Ö. Acet, N.H. Aksoy, D. Erdönmez, M. Odabaşı, Determination of some adsorption and kinetic parameters of α-amylase onto Cu+ 2-PHEMA beads embedded column, Artif. Cells Nanomed. Biotechnol. 46 (2018) S538–S545.
[31] B. Önal, Ö. Acet, R. Sanz, E.S. Sanz-Pérez, D. Erdönmez, M. Odabaşı, Co-evaluation of interaction parameters of genomic and plasmid DNA for a new chromatographic medium, Int. J. Biol. Macromol. 141 (2019) 1183–1190.
[32] F. Gurbuz, Ş. Akpınar, S. Ozcan, Ö. Acet, M. Odabaşı, Reducing arsenic and groundwater contaminants down to safe level for drinking purposes via Fe3+-attached hybrid column, Environ. Monit. Assess. 191 (2019) 1–4.
[33] S.A. Noma, Ö. Acet, A. Ulu, B. Önal, M. Odabaşı, B. Ateş, l-asparaginase immobilized p (HEMA-GMA) cryogels: a recent study for biochemical, thermodynamic and kinetic parameters, Polym. Test. 93 (2021), 106980.
[34] Ö. Acet, T. İnanan, B.Ö. Acet, E. Dikici, M. Odabaşı, α-amylase immobilized composite cryogels: some studies on kinetic and adsorption factors, Appl. Biochem. Biotechnol. 193 (2021) 2483–2496.
[35] V. Kochkodan, N. Hilal, A comprehensive review on surface modified polymer membranes for biofouling mitigation, Desalination 356 (2015) 187–207.
[36] C.J. Hawker, K.L. Wooley, The convergence of synthetic organic and polymer chemistries, Science 309 (2005) 1200–1205.
[37] W. Sun, W. Liu, Z. Wu, H. Chen, Chemical surface modification of polymeric biomaterials for biomedical applications, Macromol. Rapid Commun. 41 (2020) 1900430.
[38] Y. Asahi, Y. Noiri, J. Miura, H. Maezono, M. Yamaguchi, R. Yamamoto, H. Azakami, M. Hayashi, S. Ebisu, Effects of the tea catechin epigallocatechin gallate on *Porphyromonas gingivalis* biofilms, J. Appl. Microbiol. 116 (2014) 1164–1171.
[39] Y. Wang, A.T. Lam, Epigallocatechin gallate and gallic acid affect colonization of abiotic surfaces by oral bacteria, Arch. Oral Biol. 120 (2020), 104922.
[40] H. Tang, S. Hao, M.F. Khan, L. Zhao, F. Shi, Y. Li, H. Guo, Y. Zou, C. Lv, J. Luo, Z. Zeng, Epigallocatechin-3-gallate ameliorates acute lung damage by inhibiting quorum-sensing-related virulence factors of *Pseudomonas aeruginosa*, Front. Microbiol. 13 (2022), 874354.
[41] H. Wang, K. Helliwell, X. You, Isocratic elution system for the determination of catechins, caffeine and gallic acid in green tea using HPLC, Food Chem. 68 (2000) 115–121.
[42] Y.A. Ibrahim, A. Musa, I.A. Yakasai, Spectrophotometric method for determination of catechins in green tea and herbal formulations, Nig. J. Pharm. Sci. 16 (2017) 25–30.
[43] S. Pandit, S. Rahimi, A. Derouiche, A. Boulaoued, I. Mijakovic, Sustained release of usnic acid from graphene coatings ensures long term antibiofilm protection, Sci. Rep. 11 (2021) 1–11.
[44] S. Pandit, V. Ravikumar, A.M. Abdel-Haleem, A. Derouiche, V.R. Mokkapati, C. Sihlbom, K. Mineta, T. Gojobori, X. Gao, F. Westerlund, I. Mijakovic, Low concentrations of vitamin C reduce the synthesis of extracellular polymers and destabilize bacterial biofilms, Front. Microbiol. 8 (2017) 2599.
[45] B. Lu, F. Lu, Y. Zou, J. Liu, B. Rong, Z. Li, F. Dai, D. Wu, G. Lan, In situ reduction of silver nanoparticles by chitosan-l-glutamic acid/hyaluronic acid: enhancing antimicrobial and wound-healing activity, Carbohydr. Polym. 173 (2017) 556–565.
[46] M. Odabaşı, L. Uzun, G. Baydemir, N.H. Aksoy, Ö. Acet, D. Erdönmez, Cholesterol imprinted composite membranes for selective cholesterol recognition from intestinal mimicking solution, Colloids Surf. B Biointerfaces 163 (2018) 266–274.
[47] N.Y. Baran, Ö. Acet, M. Odabaşı, Efficient adsorption of hemoglobin from aqueous solutions by hybrid monolithic cryogel column, Mater. Sci. Eng. C 73 (2017) 15–20.
[48] H. Alkan, Ş.C. Cömert, F. Gürbüz, M. Doğru, M. Odabaşı, Cu2+-attached pumice particles embedded composite cryogels for protein purification, Artif. Cells Nanomed. Biotechnol. 45 (2017) 90–97.
[49] A.R. Blanco, A. Sudano-Roccaro, G.C. Spoto, A. Nostro, D. Rusciano, Epigallocatechin gallate inhibits biofilm formation by ocular staphylococcal isolates, Antimicrob. Agents Chemother. 49 (2005) 4339–4343.
[50] S. Hao, D. Yang, L. Zhao, F. Shi, G. Ye, H. Fu, J. Lin, H. Guo, R. He, J. Li, H. Chen, EGCG-mediated potential inhibition of biofilm development and quorum sensing in *Pseudomonas aeruginosa*, Int. J. Mol. Sci. 22 (2021) 4946.